Journal of Electronic Materials (2023) 52:971–979
https://doi.org/10.1007/s11664-022-10083-1

ORIGINAL RESEARCH ARTICLE

Thermoelectric Transport Properties of Double-Filling $In_xLa_{0.25}Co_4Sb_{12}$ Skutterudite Materials

Mohamed Bashir Ali Bashir[1] · Ethar Yahya Salih[2] · Suhana Mohd Said[3] · Yuzuru Miyazaki[4] · Dhafer Abdul-Ameer Shnawah[5] · M. Nasir Bashir[6] · Imran Haider Sajid[7] · Mohamed Hamid Elsheikh[8]

Received: 4 September 2022 / Accepted: 8 November 2022 / Published online: 5 December 2022

Abstract

Filled-skutterudite materials are promising candidates for thermoelectric applications in the intermediate-temperature range to recover waste heat. In this work, mechanical alloying and spark plasma sintering (SPS) techniques were used to consolidate double-filling $In_xLa_{0.25}Co_4Sb_{12}$ ($x = 0, 0.1, 0.3, 0.5$) samples. X-ray diffraction, scanning electron microscopy, and energy-dispersive x-ray spectroscopy were used to analyze the microstructure of the $In_xLa_{0.25}Co_4Sb_{12}$ SPS-ed samples. The microstructure results revealed the main phase of the $CoSb_3$ skutterudite structure with a small amount of InSb and $CoSb_2$ attributed to secondary phases. Electrical resistivity remarkably decreased to 9.7 μΩ m at room temperature for the $In_{0.5}La_{0.25}Co_4Sb_{12}$ sample, mainly due to the effective impurity of the InSb nanoinclusions. Moreover, the InSb nanoinclusions yielded a substantial depression in lattice thermal conductivity due to phonon scattering. The reduction in lattice thermal conductivity was approximately 62% for the $In_{0.5}La_{0.25}Co_4Sb_{12}$ sample compared with the $La_{0.25}Co_4Sb_{12}$ sample, resulting in a remarkable enhancement in the dimensionless figure-of-merit (*ZT*) of 1.25.

Keywords Mechanical alloying · thermoelectric · skutterudite · double-filling · InSb nanoinclusions

Introduction

In recent decades, thermoelectric (TE) applications have become a promising technology for energy harvesting.[1] Waste heat can be converted into useful energy via TE generation.[2] A skutterudite TE material is a good candidate for TE materials in the temperature range of 300–800 K. Furthermore, filled-skutterudite TE materials have a low lattice thermal conductivity, excellent mechanical strength, and good thermal, oxidation, and chemical stability.[3] However, the binary skutterudite $CoSb_3$ system may not be suitable for TE applications, owing to its low carrier concentration, high electrical resistivity, and high thermal conductivity.[4] Generally, carrier effective mass, carrier concentration, and carrier mobility play an important role in TE characteristics. Three different approaches are used to improve skutterudite TE material: filling the voids,[5–7] doping or substitution at antimony or cobalt sites,[8,9] and nanostructuring.[10–12]

A heavy filler atom is a promising strategy to enhance the performance of skutterudite systems, owing to its high carrier concentration and low lattice thermal conductivity. In general, the atomic radius of the filler should be smaller than the void radius of skutterudite Co_4Sb_{12} (1.892 Å)[13,14]

✉ Mohamed Bashir Ali Bashir
mbashir@ju.edu.sa; mbabashir3@gmail.com

1 Department of Mechanical Engineering, College of Engineering, Jouf University, Sakaka 42421, Saudi Arabia

2 Department of Medical Physics, College of Medical Sciences Technology, The University of Mashreq, Baghdad 10021, Iraq

3 Department of Electrical Engineering, University of Malaya, 50603 Kuala Lumpur, Malaysia

4 Department of Applied Physics, Graduate School of Engineering, Tohoku University, 6-6-05 Aoba, Aramaki, Aoba-Ku, Sendai 980-8579, Japan

5 School of Engineering, Faculty of Science and Engineering, Macquarie University, Balaclava Rd, Macquarie Park, Sydney, NSW 2109, Australia

6 National University of Sciences and Technology, Islamabad, Pakistan

7 Physics Characterization and Simulation Lab, School of Natural Sciences, National University of Sciences and Technology, Islamabad 44000, Pakistan

8 Department of Mechanical Engineering, University of Bahri, 13104 Khartoum, Sudan

to be easily filled into the void space. Several experiments have been conducted on skutterudite materials by adding fillers, such as Ba, Bi, Ce, Hf, In, La, Li, Sr, Tl, and Yb,[15–25] and the TE properties improved by enhancing the carrier concentration and mobility, as well as minimizing the lattice thermal conductivity. For example, Li et al.[26] investigated the effect of In-filling into skutterudite material. They found that In addition increased the carrier concentration due to the supply of electrons. The thermoelectric figure-of-merit (*ZT*) increased to the highest value of 0.67 for $In_{0.35}Co_4Sb_{12}$ at 600 K. Sesselmann et al.[27] examined the effect of changing the heat treatment parameters on In-filled skutterudite. The results showed a major reduction in lattice thermal conductivity due to minor changes in the synthesis parameters. Consequently, the maximum value *ZT* of 0.7 for the $In_{0.2}Co_4Sb_{12}$ sample at 675 K was achieved. Deng et al.[28] studied $In_xCo_4Sb_{12}$ -filled skutterudite compounds. The results showed the highest power factor of 31.3 μW/cmK^2 at 616 K and the lowest thermal conductivity of 2.193 W/mK at 568 K. The enhanced dimensionless *ZT* was 0.88 for the $In_{0.5}Co_4Sb_{12}$ sample at 665 K. Mallik et al. studied the influence of In addition into a Co_4Sb_{12} compound. The results showed a considerable reduction in thermal conductivity probably due to the rattling of In-filling and the presence of InSb as the secondary phase at the grain boundaries. The thermoelectric *ZT* achieved the highest values of 1.12 and 0.96 for the $In_{0.25}Co_4Sb_{12}$ and $In_{0.4}Co_4Sb_{12}$ compounds, respectively.[29,30] The same compound of $In_{0.25}Co_4Sb_{12}$ filling skutterudite was obtained by He et al.[31] who achieved a high *ZT* of 1.2 at 575 K. Lee et al.[32] studied multi-filled skutterudite $In_xYb_yLa_{0.3-x-y}Co_4Sb_{12}$ compounds. The results showed that the double-filling skutterudite was most effective in reducing thermal conductivity. A maximum *ZT* of 0.9 was obtained for the $In_{0.1}Yb_{0.2}Co_4Sb_{12}$ sample at 782 K. Khovaylo et al.[33] investigated the effect of In-filled skutterudite. The results showed a substantial contribution of phonon scattering due to the InSb impurity phase that precipitated in nanometer-sized regions along the grain boundaries, and, consequently, a considerable reduction in a thermal conductivity. Thus, a maximum $ZT \approx 1.5$ was recorded for the $In_1Co_4Sb_{12}$ sample at 725 K.

The current work aims to investigate the double-filling of $In_xLa_{0.25}Co_4Sb_{12}$ materials to boost the carrier concentration and improve the TE transport properties. A double-filled skutterudite system was synthesized with La as the dominating filling element and In as the auxiliary filler. The In atom can successfully fill the $La_{0.25}Co_4Sb_{12}$ skutterudite void because the atomic radius of In (1.55 Å) is smaller than the void radius of skutterudite Co_4Sb_{12} (1.892 Å).[13] The results show a remarkable reduction in lattice thermal conductivity for the $In_{0.5}La_{0.25}Co_4Sb_{12}$ sample compared with the $La_{0.25}Co_4Sb_{12}$ sample.

Experimental

Sample Preparation and Measurements

High-purity powder of Co (99.8%), Sb (99.5%), La (99.9%), and In (99.99%) were purchased from Alfa Aesar, and all the preparation processes are discussed in the literature.[34] The samples were cut into various parts for characterization. X-ray diffraction (XRD), scanning electron microscopy (SEM), and energy-dispersive x-ray spectroscopy (EDX) measurement data were collected for the SPS-ed samples. The setup of the characterization devices is described in the literature.[34,35]

The temperature dependency of electrical resistivity and Seebeck coefficient was measured using a commercial instrument (ZEM-3; Ulvac-Riko), and thermal diffusivity was measured using a laser flash apparatus (TC-7000H; Ulvac-Riko). The thermal conductivity was calculated from the thermal diffusivity, D, and specific heat, C_p, using $k = D\ C_p\ d$, where d is the sample density. All the TE properties were measured at a temperature range between 300 and 800 K, and then the *ZT* value was calculated.

Results and Discussion

Microstructure Analysis of $In_xLa_{0.25}Co_4Sb_{12}$ ($0 \le x \le 0.5$) Skutterudites

Figure 1 shows the XRD patterns of the $In_xLa_{0.25}Co_4Sb_{12}$ SPS-ed samples. The analysis of XRD patterns revealed the major phase of $CoSb_3$ skutterudite for all SPS-ed samples.

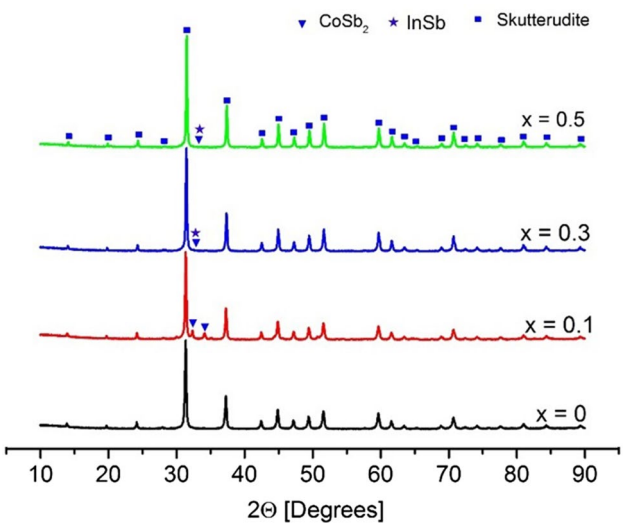

Fig. 1 XRD patterns of $In_xLa_{0.25}Co_4Sb_{12}$ ($0 \le x \le 0.5$) samples.

A small peak of impurity corresponded to $CoSb_2$ secondary phase. The formation of $CoSb_2$ phase was mainly due to the deficiency of the Sb atom and the short SPS sintering time. Moreover, the structural studies found a peak corresponding to the InSb nanoinclusion phase, as shown in Fig. 1. This nanoinclusion impurity began to occur when $x \geq 0.3$, due to the excess In in the skutterudite structure. This result agrees with previous experimental research, which revealed that the maximum limit of In-filling into the $CoSb_3$ cages is 1.37 at.% ($x = 0.22$).[30,36] Furthermore, the Rietveld refinement for the $In_xLa_{0.25}Co_4Sb_{12}$ ($0.1 \leq x \leq 0.5$) samples demonstrated the skutterudite lattice structure obtained by using Jana software, as shown in Fig. 2. The results show the lattice parameters increased from 9.0411 Å for the $La_{0.25}Co_4Sb_{12}$ sample to 9.0580 Å for the $In_{0.3}La_{0.25}Co_4Sb_{12}$ sample. Thus, the In atom successfully filled the skutterudite void because the atomic radius of In (1.55 Å) was smaller than the void radius of skutterudite Co_4Sb_{12} (1.892 Å).[13] The results of the lattice parameters and the nominal and actual compositions of the SPS-ed samples are listed in Table I.

The SEM morphologies of the $In_xLa_{0.25}Co_4Sb_{12}$ ($0.1 \leq x \leq 0.5$) SPS-ed samples are shown in Figs. 3a, 4, and 5(a). The samples exhibited a relatively high density of up to

Table I Lattice parameters, nominal and actual compositions of SPS-ed samples

Nominal composition	Actual compositions	Lattice parameter (Å)
Co_4Sb_{12}		9.0350[1]
$La_{0.25}Co_4Sb_{12}$	$La_{0.25}Co_4Sb_{12}$	9.0411 (3)
$In_{0.1}La_{0.25}Co_4Sb_{12}$	$In_{0.1}La_{0.25}Co_4Sb_{12}$	9.0453 (3)
$In_{0.3}La_{0.25}Co_4Sb_{12}$	$In_{0.31}La_{0.25}Co_4Sb_{12}$	9.0580 (2)
$In_{0.5}La_{0.25}Co_4Sb_{12}$	$In_{0.48}La_{0.25}Co_4Sb_{12}$	9.0574 (2)

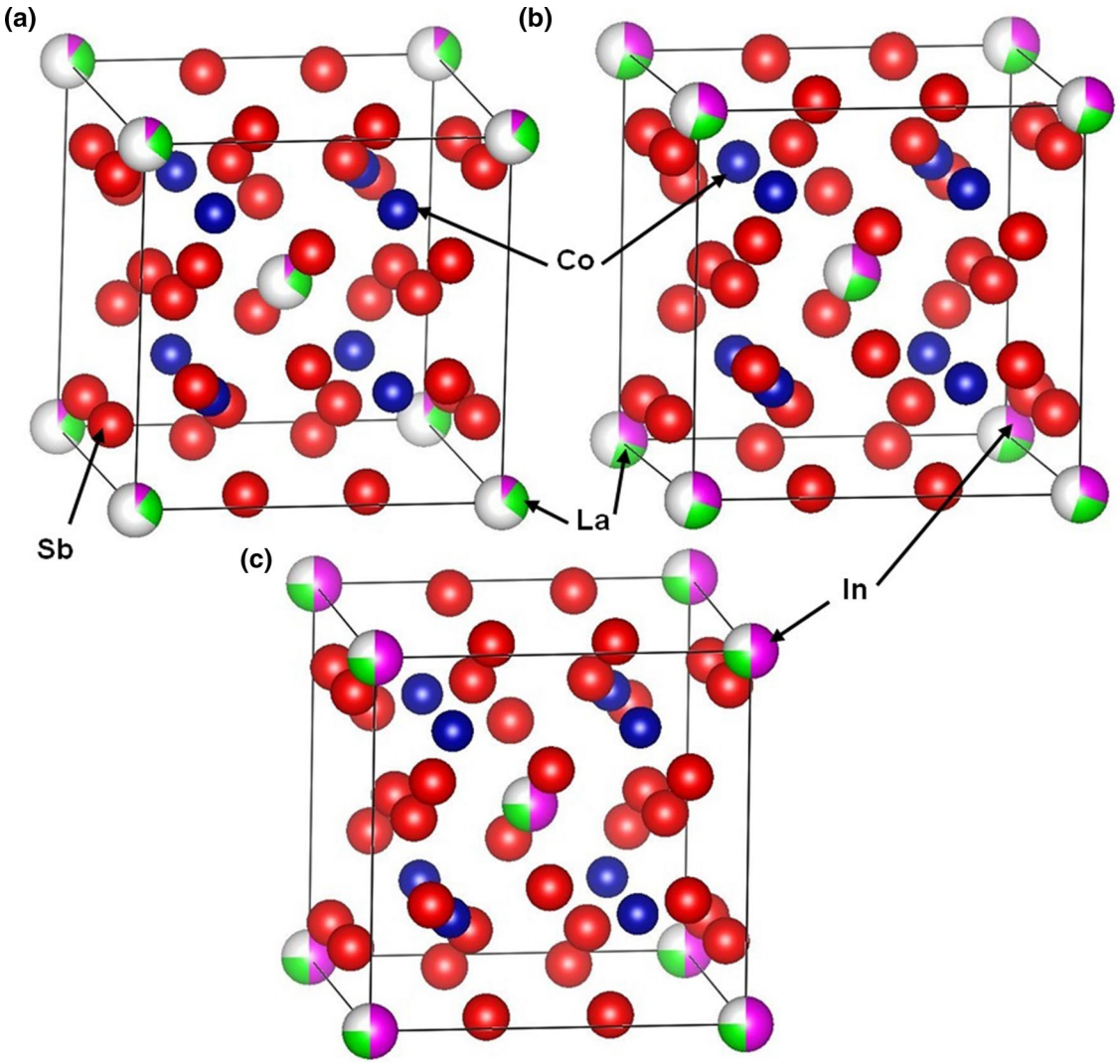

Fig. 2 Jana refinement analysis of (a) $In_{0.1}La_{0.25}Co_4Sb_{12}$, (b) $In_{0.3}La_{0.25}Co_4Sb_{12}$, and (c) $In_{0.5}La_{0.25}Co_4Sb_{12}$ SPS-ed samples.

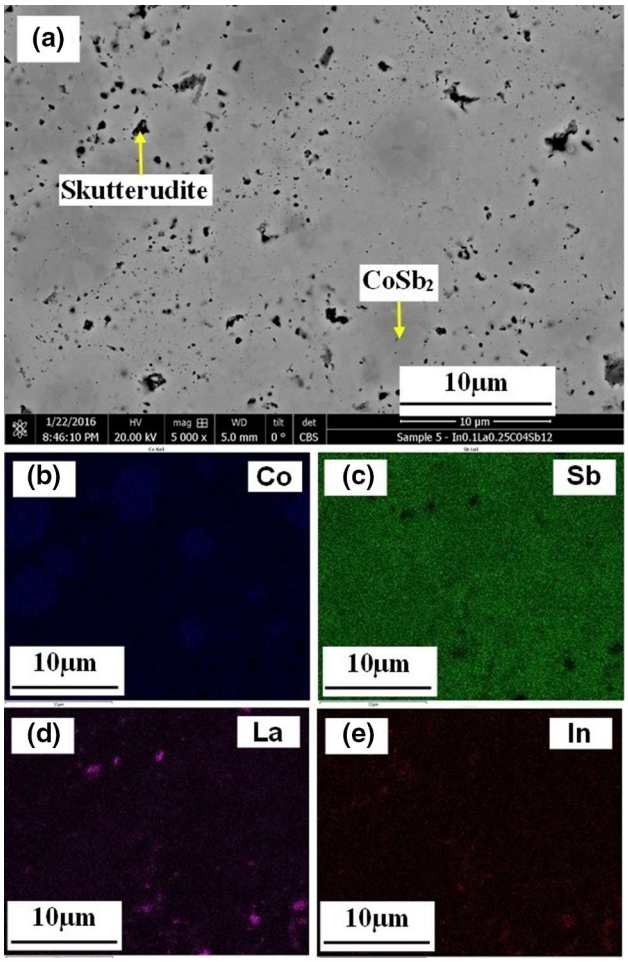

Fig. 3 (a) SEM morphology, and (b–e) corresponding elemental mappings of the $In_{0.1}La_{0.25}Co_4Sb_{12}$ SPS-ed sample.

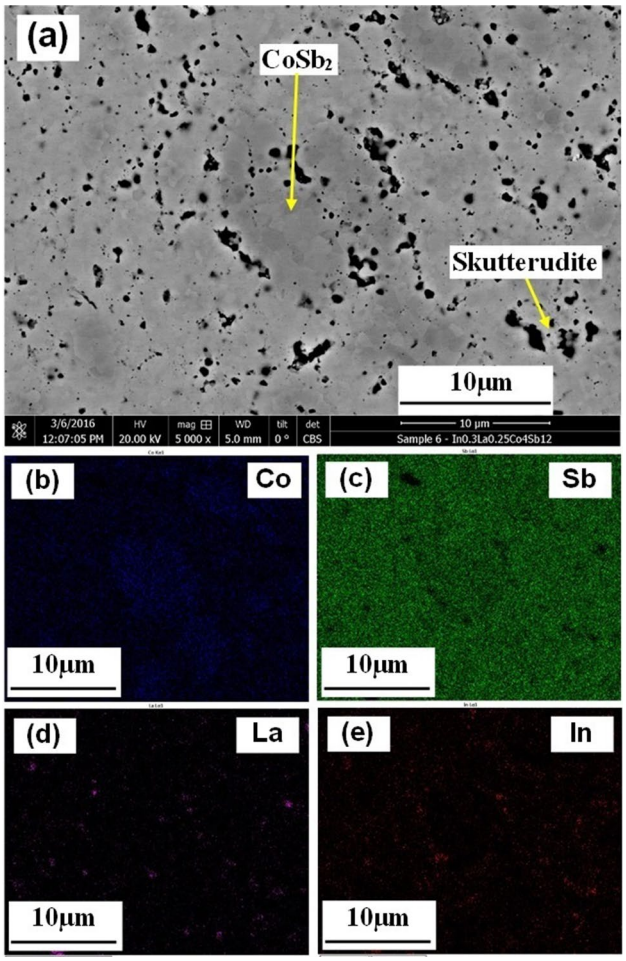

Fig. 4 (a) SEM morphology, and (b–e) corresponding elemental mappings of the $In_{0.3}La_{0.25}Co_4Sb_{12}$ SPS-ed sample.

99% according to the microstructures. However, pores were produced during SPS sintering, as evidenced by the surface morphology of the $In_{0.1}La_{0.25}Co_4Sb_{12}$ sample, which had the lowest density of about 95%. The SEM–EDX images showed skutterudite $CoSb_3$ as the primary phase for all SPS-ed samples, as well as $CoSb_2$ corresponding to the secondary phase, which match the XRD results. Moreover, the SEM–EDX results reveal that the InSb nanoinclusions were randomly distributed on the skutterudite matrix and agglomerated at the grain boundaries for the $In_{0.5}La_{0.25}Co_4Sb_{12}$ sample, as shown in Fig. 5a and d. Furthermore, the formation of the InSb nanoinclusions had a strong influence on reducing the lattice thermal conductivity due to the scattering of the charge carriers at the interfaces. Additionally, the La atoms were inhomogeneously distributed and appeared in all the samples, as shown by the elemental mapping in Figs. 3d, 4, and 5d, which may effectively scatter the phonons to further decrease the lattice thermal conductivity.[37–40]

Thermoelectric Properties

The temperature dependency of electrical resistivity for the $In_xLa_{0.25}Co_4Sb_{12}$ SPS-ed samples is shown in Fig. 6. At room temperature, the electrical resistivity rapidly decreased with increasing the In–filler fraction content, which clearly indicated that the In-filler acted as *n*-type to increase the electron concentration and that more electrons were donated to the conduction band. Furthermore, the electrical resistivity of the $In_{0.1}La_{0.25}Co_4Sb_{12}$ sample decreased with the increasing temperature, indicating non-degenerate semiconducting transport behavior, whereas, for the higher In content of the $In_{0.3}La_{0.25}Co_4Sb_{12}$ and $In_{0.5}La_{0.25}Co_4Sb_{12}$ samples, the electrical resistivity increased with temperature, displaying semimetal-like behavior. These results are consistent with published reports for skutterudites.[41,42] The InSb phase was highly conductive,[30,43] and, on reaching the solubility limit of In ($x = 0.22$), a substantial reduction in the electrical resistivity was achieved mainly due to the increasing volume fraction of InSb. Thus, the lowest

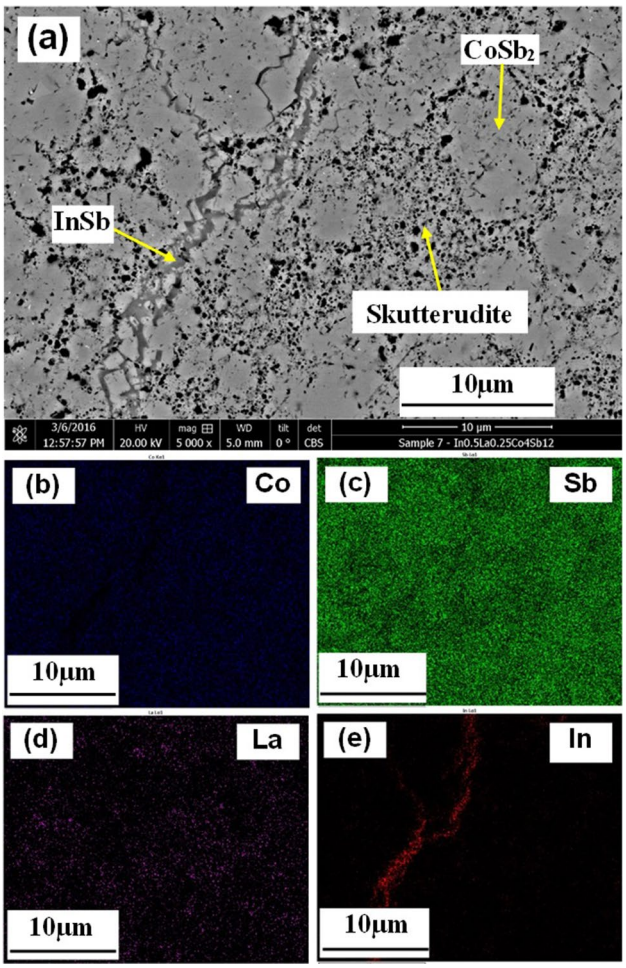

Fig. 5 (a) SEM morphology, and (b–e) corresponding elemental mappings of the $In_{0.5}La_{0.25}Co_4Sb_{12}$ SPS-ed sample.

electrical resistivity value of 9.67 µΩ m was obtained for the $In_{0.5}La_{0.25}Co_4Sb_{12}$ sample at room temperature, which was lower than that reported by He et al.[31] for $In_{0.25}Co_4Sb_{12}$, approximately 12 µΩ m at the same temperature due to the existence of the InSb phase with relatively high conductivity, as described above. Moreover, this reduction in electrical resistivity was attributed to the contribution of the In-filler atoms that acted as electron donor on the $CoSb_3$ skutterudite system that increased the carrier concentration. Additionally, the addition of In above the filling fraction limit ($x > 0.22$) saturated the material and allowed the formation of the InSb nanoinclusion phase at the grain boundaries of the Co_4Sb_{12} skutterudite matrix, as the results showed a considerable reduction in the electrical resistivity.

Figure 7 shows the variation of the Seebeck coefficient versus temperature difference for the $In_xLa_{0.25}Co_4Sb_{12}$ SPS-ed samples. Over the entire studied temperature range, all the double-filled samples showed a negative Seebeck coefficient, indicating that the *n*-type semiconductor behavior and the majority carriers were electrons. However, the Seebeck coefficient results of the single-filler $La_{0.25}Co_4Sb_{12}$ sample revealed a positive sign (*p*-type) semiconducting material, and these tendencies agreed well with the literature data[44] with the La fraction content form (0.1–0.5). Moreover, the In atoms acted as electron donors that led to decreasing the hole concentration of the $La_{0.25}Co_4Sb_{12}$ *p*-type skutterudite. The electrical conductivity of the In-filled skutterudites was inversely proportional to the Seebeck coefficients. Furthermore, the absolute Seebeck coefficient decreased with the In–filling fraction at room temperature, whereas the electrical conductivity increased owing to the higher electron carrier concentrations. The Seebeck coefficient almost monotonically increased with the temperature for $x = 0.3$ and

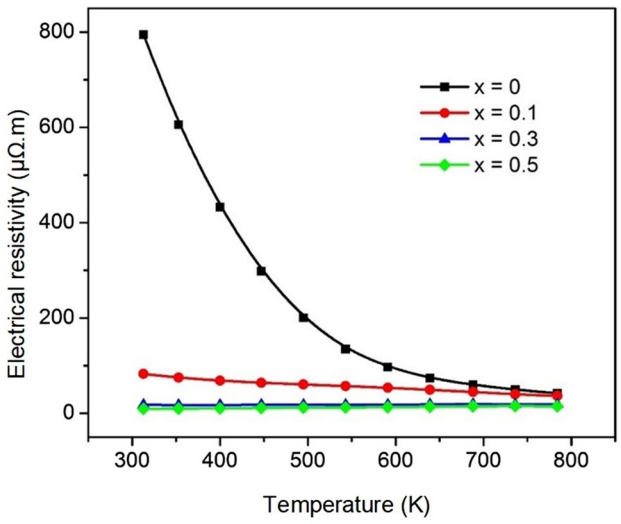

Fig. 6 Electrical resistivity for $In_xLa_{0.25}Co_4Sb_{12}$ ($0 \le x \le 0.5$) SPS-ed samples.

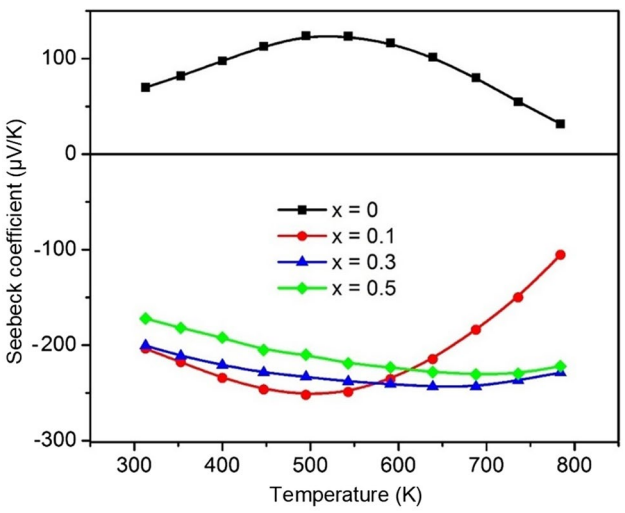

Fig. 7 Seebeck coefficient for $In_xLa_{0.25}Co_4Sb_{12}$ ($0 \le x \le 0.5$) SPS-ed samples.

$x = 0.5$. However, a nonmonotonic behavior was revealed for the $x = 0.1$ sample, hence achieving a maximum value of the Seebeck coefficient over recorded samples of 252 μVK^{-1} at 495 K. This value is higher than the 205 μVK^{-1} at 673 K obtained for the $In_{0.4}Co_4Sb_{12}$ compound.[30] Visnow[45] found that the Seebeck coefficient for the $In_{0.113}Co_4Sb_{12}$ compound was ~ 255 μVK^{-1} at 623 K, which is almost similar to the current values. However, the InSb nanoinclusion phase had a negative influence on the Seebeck coefficient, mainly due to its high conductivity, as mentioned above, and this agreed with previous published articles.[30,43]

The temperature dependency of the power factor for the $In_xLa_{0.25}Co_4Sb_{12}$ SPS-ed samples is presented in Fig. 8. The power factor can be calculated by using the equation $PF = S^2\sigma$, where S is the Seebeck coefficient, and σ is the electrical conductivity. The power factor was considerably improved with In-addition fraction content, and also the temperature, with the highest peak before declining for all samples. The highest power factor value of 3.85 10^{-3} W/mK^2 was obtained for the $In_{0.5}La_{0.25}Co_4Sb_{12}$ sample at 543 K, mainly due to the considerable reduction in electrical resistivity. This result is higher than that reported in the literature of 3.25 10^{-3} W/mK^2 for the $In_{0.3}La_{0.5}Co_4Sb_{12}$ compound at the same temperature,[46] 3.5 10^{-3} W/mK^2 for the $In_{0.25}Co_{3.9}La_{0.1}Sb_{12}$ compound at 600 K,[47] ~ 3.2 10^{-3} W/mK^2 for $In_{0.1}Yb_{0.1}La_{0.1}Co_4Sb_{12}$ compound,[48] and 2.33 10^{-3} W/mK^2 for $In_{0.05}Pr_{0.05}Co_4Sb_{12}$ at 609 K.[42]

Figure 9(a) shows the temperature dependency of the $In_xLa_{0.25}Co_4Sb_{12}$ samples as a function of thermal conductivity (k). The thermal conductivity was considerably reduced and showed nonmonotonic behavior with increasing In–filling fraction content. The lowest value of thermal conductivity of 1.27 W/mk was obtained for the $In_{0.1}La_{0.25}Co_4Sb_{12}$ sample at 495 K, which is substantially lower than the reported values of 1.6 W/mk for the $In_{0.05}Co_4Sb_{12}$ compound at 580 K.[31] This result is mainly attributed to the highest porosity of the $In_{0.1}La_{0.25}Co_4Sb_{12}$ sample, which is consistent with the literature.[49–51] For the higher In–addition fraction content ($x = 0.3$ and $x = 0.5$) samples, the thermal conductivity was high mainly due to the existence of InSb impurities with a high thermal conductivity ~ 40 W/mK.[30,43] The temperature dependency of lattice thermal conductivity (k_l) for the $In_xLa_{0.25}Co_4Sb_{12}$ samples is shown in Fig. 9b. The equation $k_l = k_{total} - k_e$ is used to compute the lattice thermal conductivity, where k_e is the electronic contribution, and k_{total} is the total thermal conductivity. Moreover, the Wiedemann–Franz law ($k_e = L.\sigma.T$, where $L = 2.44$ 10^{-8} V^2/K^2), can be used to determine the electronic contribution. The Lorenz number as the function of temperature dependence can be calculated via a single parabolic band model equation [52]:

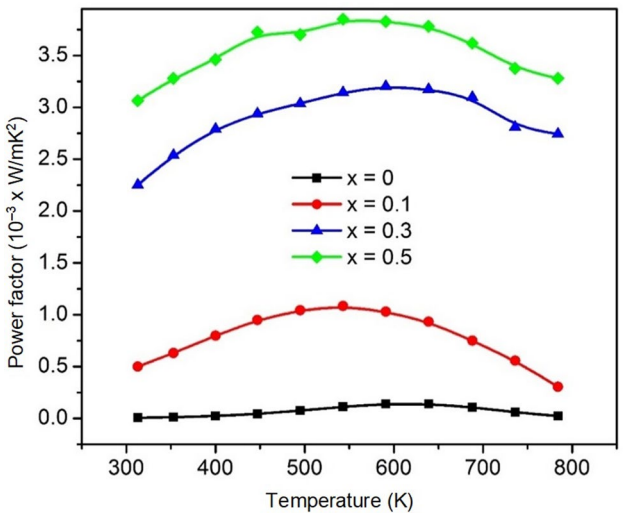

Fig. 8 Power factor for $In_xLa_{0.25}Co_4Sb_{12}$ ($0 \le x \le 0.5$) SPS-ed samples.

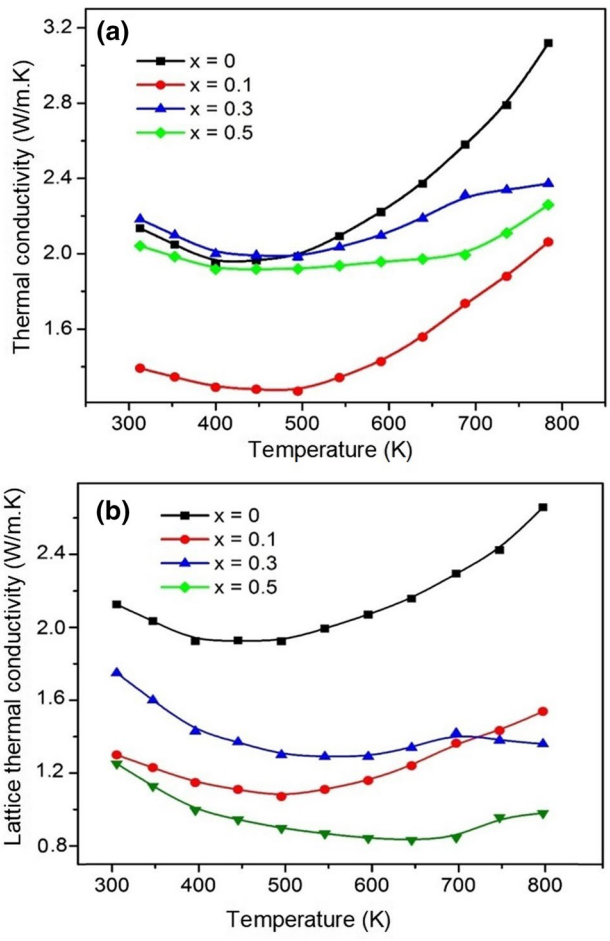

Fig. 9 (a) Thermal conductivity and (b) lattice thermal conductivity for $In_xLa_{0.25}Co_4Sb_{12}$ ($0 \le x \le 0.5$) SPS-ed samples.

$$L(T) = \left(\frac{K_B}{e}\right)^2 \left[\frac{\left(\lambda + 7/2\right) F_{\lambda+5/2}(\xi)}{\left(\lambda + 3/2\right) F_{\lambda+1/2}(\xi)} - \left(\frac{\left(\lambda + 5/2\right) F_{\lambda+3/2}(\xi)}{\left(\lambda + 3/2\right) F_{\lambda+1/2}(\xi)} \right)^2 \right], \quad (1)$$

where K_B is the Boltzmann constant, e is the electron charge, λ is the scattering parameter, $\xi = E_F/K_BT$ is the reduced Fermi energy, E_F is the Fermi energy, and $F_n(\xi)$ is the Fermi integral defined by:

$$F_n(\xi) = \int_0^\infty \frac{x^n}{1 + e^{x-\xi}} dx \quad (2)$$

In this calculation, the scattering parameter is set to be − 0.5 by assuming the acoustic phonon scattering is the dominant carrier scattering mechanism at the measurement temperature range. The reduced Fermi energy is extracted from the measured Seebeck coefficient values using[52]:

$$S = \pm \frac{K_B}{e} \left[\frac{\left(\lambda + 5/2\right) F_{\lambda+3/2}(\xi)}{\left(\lambda + 3/2\right) F_{\lambda+1/2}(\xi)} - \xi \right] \quad (3)$$

By using the extracted reduced Fermi energy, the Lorenz numbers were calculated to be 2.08, 1.61, 1.62, and 1.67×10^{-8} V^2/K^2 for the proportions of $x = 0$, 0.1, 0.3, and 0.5, respectively, at room temperature. In general, the calculated Lorenz numbers are smaller than the degenerate limit of the Lorenz number (2.44×10^{-8} V^2/K^2) typically observed in TE materials with carrier concentrations between generate and non-degenerate semiconductors. The lattice thermal conductivity parameters were considerably reduced with the In–addition fraction content. Furthermore, the InSb nanoinclusion phase induced more interfaces into the system, which led to a substantial decrease in the lattice thermal conductivity through the interface scattering of phonons. The results show ~ 62% reduction of the lattice thermal conductivity compared with the $La_{0.25}Co_4Sb_{12}$ sample. The lowest value of lattice thermal conductivity, 0.83 W/m K, was achieved for the $In_{0.5}La_{0.25}Co_4Sb_{12}$ sample at 639 K, which is three times lower than that of samples selected from the published reports.[53,54] The lowest value of lattice thermal conductivity was obtained for the highest In–filling fraction content $x = 0.5$ sample, which agrees with previous published reports.[26,27,33] In addition, the lattice thermal conductivity was minimized due to the strain field scattering of high-energy phonons.[37–40] This result agrees with the previous study by Nolas et al.,[55] who found that an uneven distribution of the filler can introduce a point-defect-type phonon scattering and scatter a large spectrum of phonons.

The temperature dependency of the $In_xLa_{0.25}Co_4Sb_{12}$ SPS-ed samples as a function of the thermoelectric ZT is shown in Fig. 10. The results show a clear trend and remarkable improvement of ZT with In–filler fraction content and temperature. The formation of the InSb nanoinclusion phase at the grain boundaries of the skutterudite matrix has a substantial effect on reducing the lattice thermal conductivity, while maintaining good electrical transport properties. Consequently, the maximum $ZT = 1.25$ obtained for $In_{0.5}La_{0.25}Co_4Sb_{12}$ sample was considerably improved compared with the In-free $La_{0.25}Co_4Sb_{12}$ sample. This result is higher than the 0.79 obtained for the $In_{0.1}Co_4Sb_{12}$ compound,[56] 0.9 attained in the $In_{0.1}Yb_{0.2}Co_4Sb_{12}$ compound at 782 K[32] and ~ 1.2 obtained for $In_{0.25}Co_4Sb_{12}$ compound.[31] The In-filler boosts the TE properties of $La_{0.25}Co_4Sb_{12}$ skutterudite material at a medium-temperature range.

Conclusions

MA and SPS techniques were used to successfully fabricate $In_xLa_{0.25}Co_4Sb_{12}$ skutterudite compounds. The major phase of the $CoSb_3$ skutterudite structure was observed by the XRD patterns for SPS-ed samples with minor amounts of $CoSb_2$ and InSb as the secondary phases. The InSb nanoinclusion impurity remarkably reduced the electrical resistivity and lattice thermal conductivity of the $In_xLa_{0.25}Co_4Sb_{12}$ skutterudites. The $In_{0.5}La_{0.25}Co_4Sb_{12}$ sample achieved the lowest electrical resistivity and lattice thermal conductivity of 9.67 μΩ m and 0.83 W/m K, respectively. Furthermore, the In-filler dramatically boosted the power factor, reaching a maximum value of 3.85 10^{-3} W/m K^2 at 543 K for the $In_{0.5}La_{0.25}Co_4Sb_{12}$ sample due to a considerable reduction in

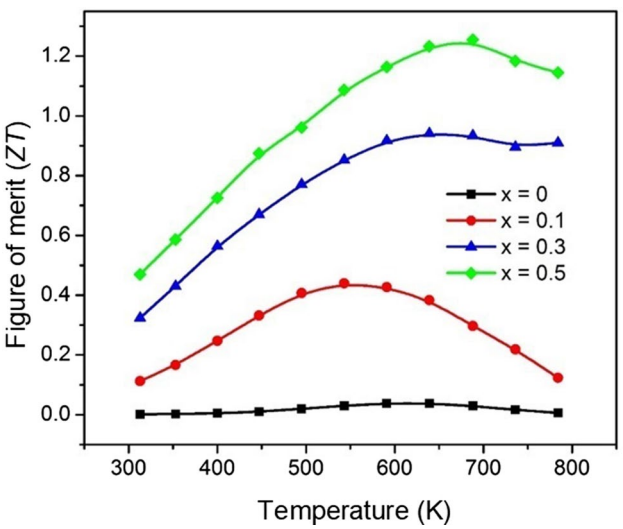

Fig. 10 The dimensionless figure of merit for $In_xLa_{0.25}Co_4Sb_{12}$ ($0 \le x \le 0.5$) SPSed samples.

electrical resistivity. The *ZT* was greatly improved to 1.25 at 688 K for the $In_{0.5}La_{0.25}Co_4Sb_{12}$ sample, which was substantially higher than that of the unfilled sample.

Acknowledgments This work was funded by the Deanship of Scientific Research at Jouf University under grant No. (DSR-2021-02-03107).

Conflict of interest All authors have no conflict of interest.

References

1. M.B.A. Bashir, S. Mohd Said, M.F.M. Sabri, D.A. Shnawah, and M.H. Elsheikh, Recent advances on $Mg_2Si_{1-x}Sn_x$ materials for thermoelectric generation. *Renew. Sustain. Energy Rev.* 37, 569–584 (2014).
2. M. Hamid Elsheikh, D.A. Shnawah, M.F.M. Sabri, S.B.M. Said, M. Haji Hassan, M.B. Ali Bashir, and M. Mohamad, A review on thermoelectric renewable energy: principle parameters that affect their performance. *Renew. Sustain. Energy Rev.* 30, 337–355 (2014).
3. D.Y.N. Truong, H. Kleinke, and F. Gascoin, Thermoelectric properties of higher manganese silicide/multi-walled carbon nanotube composites. *J. Chem. Soc. Dalt. Trans.* 43, 15092–15097 (2014).
4. K.H. Park, S.C. Ur, I.H. Kim, S.M. Choi, and W.S. Seo, Transport properties of Sn-doped $CoSb_3$ skutterudites. *J. Korean Phys. Soc.* 57, 1000–1004 (2010).
5. J.L. Feldman, P. Dai, T. Enck, B.C. Sales, D. Mandrus, and D.J. Singh, Lattice vibrations in La(Ce)Fe_4Sb_{12} and $CoSb_3$: Inelastic neutron scattering and theory. *Phys. Rev. B.* 73, 14306 (2006).
6. V. Keppens, D. Mandrus, B.C. Sales, B.C. Chakoumakos, P. Dai, R. Coldea, M.B. Maple, D.A. Gajewski, E.J. Freeman, and S. Bennington, Localized vibrational modes in metallic solids. *Nature* 395, 876–878 (1998).
7. M.M. Koza, M.R. Johnson, R. Viennois, H. Mutka, L. Girard, and D. Ravot, Breakdown of phonon glass paradigm in La-and Ce-filled Fe_4Sb_{12} skutterudites. *Nat. Mater.* 7, 805–810 (2008).
8. J. Yang, D.T. Morelli, G.P. Meisner, W. Chen, J.S. Dyck, and C. Uher, Effect of Sn substituting for Sb on the low-temperature transport properties of ytterbium-filled skutterudites. *Phys. Rev. B.* 67, 165207 (2003).
9. Z. Zhou, C. Uher, A. Jewell, and T. Caillat, Influence of point-defect scattering on the lattice thermal conductivity of solid solution $Co(Sb_{1-x}As_x)_3$. *Phys. Rev. B.* 71, 235209 (2005).
10. Y. Tang, Z.M. Gibbs, L.A. Agapito, G. Li, H.-S. Kim, M.B. Nardelli, S. Curtarolo, and G.J. Snyder, Convergence of multi-valley bands as the electronic origin of high thermoelectric performance in $CoSb_3$ skutterudites. *Nat. Mater.* 14, 1223–1228 (2015).
11. M. Rull-Bravo, A. Moure, J.F. Fernández, and M. Martín-González, Skutterudites as thermoelectric materials: revisited. *Rsc Adv.* 5, 41653–41667 (2015).
12. J.W. Sharp, E.C. Jones, R.K. Williams, P.M. Martin, and B.C. Sales, Thermoelectric properties of $CoSb_3$ and related alloys. *J. Appl. Phys.* 78, 1013–1018 (1995).
13. J.C. Slater, Structure of isobutylene. *J. Chem. Phys.* 41, 3199 (1964).
14. V. Trivedi, M. Battabyal, P. Balasubramanian, G.M. Muralikrishna, P.K. Jain, and R. Gopalan, Microstructure and doping effect on the enhancement of the thermoelectric properties of Ni doped Dy filled $CoSb_3$ skutterudites. *Sustain. Energy Fuels.* 2, 2687–2697 (2018).
15. G. Rogl, A. Grytsiv, P. Rogl, N. Peranio, E. Bauer, M. Zehetbauer, and O. Eibl, N-type skutterudites (R, Ba, Yb)$_y$$Co_4Sb_{12}$ (R = Sr, la, mm, DD, SrMm, SrDD) approaching ZT≈ 2.0. *Acta Mater.* 63, 30–43 (2014).
16. L.D. Chen, T. Kawahara, X.F. Tang, T. Goto, T. Hirai, J.S. Dyck, W. Chen, and C. Uher, Anomalous barium filling fraction and n-type thermoelectric performance of $Ba_yCo_4Sb_{12}$. *J. Appl. Phys.* 90, 1864–1868 (2001).
17. T. Dahal, Q. Jie, G. Joshi, S. Chen, C. Guo, Y. Lan, and Z. Ren, Thermoelectric property enhancement in Yb-doped n-type skutterudites $Yb_xCo_4Sb_{12}$. *Acta Mater.* 75, 316–321 (2014).
18. H. Li, X. Su, X. Tang, Q. Zhang, C. Uher, G.J. Snyder, and U. Aydemir, Grain boundary engineering with nano-scale InSb producing high performance $In_xCe_yCo_4Sb_{12+z}$ skutterudite thermoelectrics. *J. Mater.* 3, 273–279 (2017).
19. C. Chen, L. Zhang, J. Li, F. Yu, D. Yu, Y. Tian, and B. Xu, Enhanced thermoelectric performance of lanthanum filled $CoSb_3$ synthesized under high pressure. *J. Alloys Compd.* 699, 751–755 (2017).
20. G. Tan, Y. Zheng, Y. Yan, and X. Tang, Preparation and thermoelectric properties of p-type filled skutterudites $Ce_yFe_{4-x}Ni_xSb_{12}$. *J. Alloys Compd.* 584, 216–221 (2014).
21. S. Choi, K. Kurosaki, A. Yusufu, Y. Ohishi, H. Muta, and S. Yamanaka, Thermoelectric properties of p-Type Tl-filled skutterudites: $Tl_xFe_{1.5}Co_{2.5}Sb_{12}$. *J. Electron. Mater.* 44, 1743–1749 (2015).
22. G. Rogl, A. Grytsiv, K. Yubuta, S. Puchegger, E. Bauer, C. Raju, R.C. Mallik, and P. Rogl, In-doped multifilled n-type skutterudites with ZT= 1.8. *Acta Mater.* 95, 201–211 (2015).
23. M.H. Elsheikh, M.F.M. Sabri, S.M. Said, Y. Miyazaki, H.H. Masjuki, D.A. Shnawah, N. Abdullah, S. Naito, and M.B.A. Bashir, Microstructural modification of Co_4Sb_{12} skutterudite thermoelectric material through Al exceed doping. *Sci. Adv. Mater.* 8, 2121–2127 (2016).
24. O. Raihan, S. Mohd Said, M.F.M. Sabri, S. Rozali, B.D. Long, K. Kimura, K. Tobita, M.F. Fitriani, M.B. Mohd Salleh, and Ali Bashir, Parametric analysis of ball milling condition on thermoelectric performance of $Bi_{0.6}FeCo_3Sb_{12}$ skutterudite. *Mater. Res. Exp.* 5, 105008 (2018).
25. M.H. Elsheikh, M.F.M. Sabri, S.M. Said, Y. Miyazaki, H.H. Masjuki, D.A. Shnawah, S. Naito, and M.B.A. Bashir, Rapid preparation of bulk $Al_xYb_{0.25}Co_4Sb_{12}$ (x = 0, 0.1, 0.2, 0.3) skutterudite thermoelectric materials with high figure of merit ZT = 1.36. *J. Mater. Sci.* 52, 5324–5332 (2017).
26. G. Li, K. Kurosaki, Y. Ohishi, H. Muta, and S. Yamanaka, Thermoelectric properties of indium-added skutterudites $In_xCo_4Sb_{12}$. *J. Electron. Mater.* 42, 1463–1468 (2013).
27. A. Sesselmann, T. Dasgupta, K. Kelm, E. Müller, S. Perlt, and S. Zastrow, Transport properties and microstructure of indium-added cobalt–antimony-based skutterudites. *J. Mater. Res.* 26, 1820–1826 (2011).
28. L. Deng, X.P. Jia, T.C. Su, S.Z. Zheng, X. Guo, K. Jie, and H.A. Ma, The thermoelectric properties of $In_xCo_4Sb_{12}$ alloys prepared by HPHT. *Mater. Lett.* 65, 2927–2929 (2011).
29. R.C. Mallik, J.-Y. Jung, S.-C. Ur, and I.-H. Kim, Thermoelectric properties of $In_zCo_4Sb_{12}$ skutterudites. *Met. Mater. Int.* 14, 223–228 (2008).
30. R.C. Mallik, C. Stiewe, G. Karpinski, R. Hassdorf, and E. Müller, Thermoelectric properties of Co_4Sb_{12} skutterudite materials with partial in filling and excess in additions. *J. Electron. Mater.* 38, 1337–1343 (2009).
31. T. He, J. Chen, H.D. Rosenfeld, and M.A. Subramanian, Thermoelectric properties of indium-filled skutterudites. *Chem. Mater.* 18, 759–762 (2006).
32. J.-K. Lee, S.-M. Choi, W.-S. Seo, Y.-S. Lim, H.-L. Lee, and I.-H. Kim, Thermoelectric properties of Spark Plasma Sintered $In_xYb_yLa_{0.3-x-y}Co_4Sb_{12}$ skutterudite system. *Renew. Energy.* 42, 36–40 (2012).

33. V.V. Khovaylo, T.A. Korolkov, A.I. Voronin, M.V. Gorshenkov, and A.T. Burkov, Rapid preparation of $In_xCo_4Sb_{12}$ with a record-breaking ZT= 1.5: the role of the in overfilling fraction limit and Sb overstoichiometry. *J. Mater. Chem. A.* 5, 3541–3546 (2017).
34. S.M. Said, M.B.A. Bashir, M.F.M. Sabri, Y. Miyazaki, D.A.A. Shnawah, A.S. Hakeem, M. Shimada, A.I. Bakare, N.N.N. Ghazali, and M.H. Elsheikh, Enhancement of thermoelectric behavior of $La_{0.5}Co_4Sb_{12-x}Te_x$ skutterudite materials. *Metall Mater. Trans. A Phys. Metall. Mater. Sci.* 48, 3073–3081 (2017).
35. M. Bashir, A. Bashir, S.M. Said, M. Faizul, M. Sabri, and Y. Miyazaki, Enhancement of thermoelectric properties of $Yb_{0.25}Co_4Sb_{12}$ skutterudites through Ni substitution. *Sains Malaysiana.* 47, 181–187 (2018).
36. K.I. Litvinova, A.I. Voronin, M.V. Gorshenkov, D.Y. Karpenkov, A.P. Novitskii, and V.V. Khovaylo, Thermoelectric properties of $Ce_xNd_yCo_4Sb_{12}$ skutterudites. *Semiconductors* 51, 928–931 (2017).
37. H. Geng, J. Zhang, T. He, L. Zhang, and J. Feng, Microstructure evolution and mechanical properties of melt spun skutterudite-based thermoelectric materials. *Materials (Basel).* 13, 984 (2020).
38. R. Wei, G. Huiyuan, Z. Zihao, and Z. Lixia, Filling-fraction fluctuation leading to glasslike ultralow thermal conductivity in caged skutterudites. *Phys. Rev. Lett.* 118, 245901 (2017).
39. J. Gainza, F. Serrano-Sánchez, J. Prado-Gonjal, N.M. Nemes, N. Biskup, O.J. Dura, J.L. Martínez, F. Fauth, and J.A. Alonso, Substantial thermal conductivity reduction in mischmetal skutterudites $Mm_xCo_4Sb_{12}$ prepared under high-pressure conditions, due to uneven distribution of the rare-earth elements. *J. Mater. Chem. C.* 7, 4124–4131 (2019).
40. X. Tong, Z. Liu, J. Zhu, T. Yang, Y. Wang, and A. Xia, Research progress of p-type Fe-based skutterudite thermoelectric materials. *Front. Mater. Sci.* 15, 1–17 (2021).
41. G. Tang, D. Zhang, G. Chen, F. Xu, and Z. Wang, High temperature thermoelectric and magnetic properties of $In_xNd_yCo_4Sb_{12}$ skutterudites. *Phys. B Condens. Matter.* 408, 79–82 (2013).
42. G. Tang, W. Yang, F. Xu, and Y. He, Synthesis and thermoelectric properties of In and Pr double-filled skutterudites $In_xPr_yCo_4Sb_{12}$. *J. Electron. Mater.* 43, 435–438 (2014).
43. G. Busch and E.F. Steigmier, Thermal and electrical conductivities, Hall effect and thermoelectric power of InSb. *Helv. Phys. Acta.* 34, 1–28 (1961).
44. K. Liu, X. Dong, and Z. Jiuxing, The effects of La on thermoelectric properties of $La_xCo_4Sb_{12}$ prepared by MA-SPS. *Mater. Chem. Phys.* 96, 371–375 (2006).
45. E. Visnow, C.P. Heinrich, A. Schmitz, J. De Boor, P. Leidich, B. Klobes, R.P. Hermann, W.E. Müller, and W. Tremel, On the true indium content of In-filled skutterudites. *Inorg. Chem.* 54, 7818–7827 (2015).
46. M.B.A. Bashir, S.M. Said, M.F.M. Sabri, Y. Miyazaki, D.A. Shnawah, M. Shimada, M.F.M. Salleh, M.S. Mahmood, E.Y. Salih, F. Fitriani, and M.H. Elsheikh, In-filled $La_{0.5}Co_4Sb_{12}$ skutterudite system with high thermoelectric figure of merit. *J. Electron. Mater.* 47, 2429–2438 (2018).
47. J.-Y. Jung, K.-H. Park, I.-H. Kim, S.-M. Choi, and W.-S. Seo, Thermoelectric and transport properties of in-filled and Ni-doped $CoSb_3$ skutterudites. *J. Korean Phys. Soc.* 57, 773–777 (2010).
48. J.K. Lee, S.M. Choi, W.S. Seo, Y.S. Lim, H.L. Lee, and I.H. Kim, Thermoelectric properties of spark plasma sintered $In_xYb_yLa_{0.3-x-y}Co_4Sb_{12}$ skutterudite system. *Renew. Energy.* 42, 36–40 (2012).
49. L. Yang, J.S. Wu, and L.T. Zhang, Synthesis of filled skutterudite compound $La_{0.75}Fe_3CoSb_{12}$ by spark plasma sintering and effect of porosity on thermoelectric properties. *J. Alloys Compd.* 364, 83–88 (2004).
50. N. Gostkowska-Lekner, B. Trawinski, A. Kosonowski, B. Bochentyn, M. Lapinski, T. Miruszewski, K. Wojciechowski, and B. Kusz, New synthesis route of highly porous $In_xCo_4Sb_{12}$ with strongly reduced thermal conductivity. *J. Mater. Sci.* 55, 13658–13674 (2020).
51. F. Fitriani, S.M. Said, S. Rozali, M.F. Mohd, M. Faizul, M. Sabri, L. Bui, T. Nakayama, O. Raihan, M.M.I. Megat Hasnan, M.B.A. Bashir, and F. Kamal, Enhancement of thermoelectric properties in cold pressed nickel doped bismuth sulfide compounds. *J. Electron. Mater.* 14, 689–699 (2018). https://doi.org/10.1007/s13391-018-0072-8.
52. D.M. Rowe and C.M. Bhandari, *Modern Thermoelectrics* (London: Holt. Rinehart Winst, 1983), p. 69.
53. G. Li, K. Kurosaki, Y. Ohishi, H. Muta, and S. Yamanaka, Thermoelectric properties of indium-added skutterudites $In_xCo_4Sb_{12}$. *J. Electron. Mater.* 42, 1463–1468 (2013).
54. M.B.A. Bashir, M.F. Mohd Sabri, S.M. Said, Y. Miyazaki, I.A. Badruddin, D.A. Ameer Shnawah, E.Y. Salih, S. Abushousha, and M.H. Elsheikh, Enhancement of thermoelectric properties of Co_4Sb_{12} skutterudite by Al and La double filling. *J. Solid State Chem.* 284, 121205 (2020).
55. G.S. Nolas, J.L. Cohn, and G.A. Slack, Effect of partial void filling on the lattice thermal conductivity of skutterudites. *Phys. Rev. B.* 58, 164 (1998).
56. L. Wang, K.F. Cai, Y.Y. Wang, H. Li, and H.F. Wang, Thermoelectric properties of indium-filled skutterudites prepared by combining solvothermal synthesis and melting. *Appl. Phys. A Mater. Sci. Process.* 97, 841–845 (2009).